Magnon contribution to unidirectional spin Hall magnetoresistance in ferromagnetic-insulator/heavy-metal bilayers

W. P. Sterk and D. Peerlings
Institute for Theoretical Physics, Utrecht University, Princetonplein 5, 3584 CC Utrecht, The Netherlands

R. A. Duine
Institute for Theoretical Physics, Utrecht University, Princetonplein 5, 3584 CC Utrecht, The Netherlands
and Department of Applied Physics, Eindhoven University of Technology, P. O. Box 513, 5600 MB Eindhoven, The Netherlands

(Received 18 October 2018; published 28 February 2019)

We develop a model for the magnonic contribution to the unidirectional spin Hall magnetoresistance (USMR) of heavy metal/ferromagnetic insulator bilayer films. We show that diffusive transport of Holstein-Primakoff magnons leads to an accumulation of spin near the bilayer interface, giving rise to a magnoresistance which is not invariant under inversion of the current direction. Unlike the electronic contribution described by Zhang and Vignale [Phys. Rev. B **94**, 140411 (2016)], which requires an electrically conductive ferromagnet, the magnonic contribution can occur in ferromagnetic insulators such as yttrium iron garnet. We show that the magnonic USMR is, to leading order, cubic in the spin Hall angle of the heavy metal, as opposed to the linear relation found for the electronic contribution. We estimate that the maximal magnonic USMR in Pt|YIG bilayers is on the order of 10^{-8} but may reach values of up to 10^{-5} if the magnon gap is suppressed and can thus become comparable to the electronic contribution in, e.g., Pt|Co. We show that the magnonic USMR at a finite magnon gap may be enhanced by an order of magnitude if the magnon diffusion length is decreased to a specific optimal value that depends on various system parameters.

DOI: 10.1103/PhysRevB.99.064438

I. INTRODUCTION

The total magnetoresistance of metal/ferromagnet heterostructures is known to comprise several independent contributions, including but not limited to anisotropic magnetoresistance (AMR) [1], giant magnetoresistance (GMR, in stacked magnetic multilayers) [2], and spin Hall magnetoresistance (SMR) [3]. A common characteristic of these effects is that they are linear; in particular, this means the measured magnetoresistance is invariant under reversal of the polarity of the current.

In 2015, however, Avci *et al.* [4] measured a small but distinct asymmetry in the magnetoresistance of Ta|Pt and Co|Pt bilayer films. Due to its striking similarity to the current-in-plane spin Hall effect (SHE) and GMR, save for its nonlinear resistance/current characteristic, this effect was dubbed unidirectional spin Hall magnetoresistance (USMR).

In the years following its discovery, USMR has been detected in bilayers consisting of magnetic and nonmagnetic topological insulators [5], and the dependence of the USMR on layer thickness has been investigated experimentally for Co|Pt bilayers [6]. Additionally, Avci *et al.* [7] have shown that USMR may be used to distinguish between the four distinct magnetic states of a ferromagnet|normal metal|ferromagnet trilayer stack, highlighting its potential application in multibit electrically controlled memory cells.

Although USMR is ostensibly caused by spin accumulation at the ferromagnet|metal interface, a complete theoretical understanding of this effect is lacking. In bilayer films consisting of ferromagnetic metal (FM) and heavy metal (HM) layers, electronic spin accumulation in the ferromagnet caused by spin-dependent electron mobility provides a close match to the observed results [8]. It remains unknown, however, whether this is the full story; indeed, this model's underestimation of the USMR by a factor of two lends plausibility to the idea that there may be additional, as-yet-unknown contributions providing the same experimental signature. Additionally, the electronic spin accumulation model cannot be applied to bilayers consisting of a ferromagnetic insulator (FI) and a HM, as there will be no electric current in the ferromagnet to drive accumulation of spin.

Kim *et al.* [9] have measured the USMR of Py|Pt (where Py denotes for permalloy) bilayer and claim, using qualitative arguments, that a *magnonic* process is involved. Likewise, for Co|Pt and CoCr|Pt, more recent results by Avci *et al.* [10] argue in favor of the presence of a magnon-scattering contribution consisting of terms linear and cubic in the applied current and having a magnitude comparable to the electronic contribution of Zhang and Vignale [8]. Although these experimental results provide a great deal of insight into the underlying processes, a theoretical framework against which they can be tested is presently lacking. In this work, we aim to take first steps to developing such a framework by considering an accumulation of magnonic spin near the FI|HM bilayer interface, which we describe by means of a drift-diffusion model.

The remainder of this article is structured as follows: in Sec. II, we present our analytical model as generically as possible. In Sec. III we analyze the behavior of our model using parameters corresponding to a Pt|YIG (YIG being yttrium iron garnet) bilayer as a basis. In particular, in Sec. III A we give

quantitative predictions of the magnonic USMR in terms of the applied current and layer thicknesses, and in Sec. III B we take into account the effect of Joule heating. In the remainder of Sec. III, we investigate the influence of various material parameters. Finally, in Sec. IV we summarize our key results and present some open questions.

II. MAGNONIC SPIN ACCUMULATION

To develop a model of the magnonic contribution to the USMR, we focus on the simplest FI|HM heterostructure: a homogeneous bilayer. We treat the transport of magnonic and electronic spin as diffusive and solve the resulting diffusion equations subject to a quadratic boundary condition at the interface. In this approach, valid in the opaque interface limit, current-dependent spin accumulations—electronic in the HM and magnonic in the FI—form near the interface. In particular, the use of a nonlinear boundary condition breaks the invariance of the SMR under reversal of the current direction, i.e., it produces USMR.

We consider a sample consisting of a FI layer of thickness L_{FI} directly contacting a HM layer of thickness L_{HM}. We take the interface to be the xy plane, such that the FI layer extends from $z = 0$ to L_{FI} and the HM layer from $z = -L_{\mathrm{HM}}$ to 0. The magnetization is chosen to lie in the positive y direction, and an electric field $\boldsymbol{E} = \pm E\hat{\mathbf{x}}$ is applied in the x direction. The set-up is shown in Fig. 1.

The extents of the system parallel to the interface are taken to be infinite and the individual layers completely homogeneous. This allows us to treat the system as quasi-one-dimensional in the sense that we will only consider spin currents that flow in the z direction. We account for magnetic anisotropy only indirectly through the existence of a magnon gap. We further assume that our system is adequately described by the Drude model (suitably extended to include spin effects [11]) and that the interface between layers is not fully transparent to spin current, i.e., has a finite spin-mixing conductance [12]. For simplicity, we assume electronic spin and charge transport may be neglected in the ferromagnet, as is the case for ferromagnetic insulators.

We describe the transfer of spin across the interface microscopically by the continuum-limit interaction Hamiltonian

$$H_{\mathrm{int}} = -\int d^3\boldsymbol{r}d^3\boldsymbol{r}'\, J(\boldsymbol{r},\boldsymbol{r}')[b^\dagger(\boldsymbol{r}')c^\dagger_\downarrow(\boldsymbol{r})c_\uparrow(\boldsymbol{r}) + b(\boldsymbol{r}')c^\dagger_\uparrow(\boldsymbol{r})c_\downarrow(\boldsymbol{r})],$$

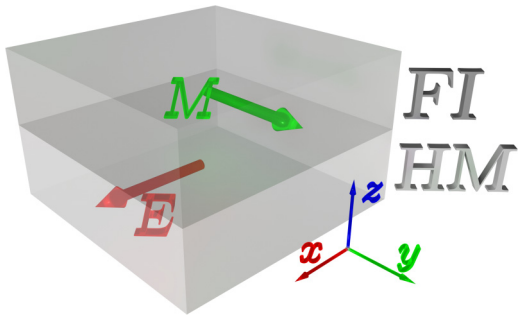

FIG. 1. Schematic depiction of our system. The magnetization M of the FI layer lies in the $+y$ direction, an electric field of magnitude E is applied to the heavy metal layer (HM) in the $\pm x$ direction, and the interface between the layers lies in the xy plane.

where $c^\dagger_\alpha(\boldsymbol{r})$ [$c_\alpha(\boldsymbol{r})$] are fermionic creation [annihilation] operators of electrons with spin $\alpha \in \{\uparrow,\downarrow\}$ at position $\boldsymbol{r}$ in the HM, and $b^\dagger(\boldsymbol{r}')$ [$b(\boldsymbol{r}')$] is the bosonic creation [annihilation] operator of a circularly polarized Holstein-Primakoff magnon [13] at position $\boldsymbol{r}'$ inside the ferromagnet. We leave $J(\boldsymbol{r},\boldsymbol{r}')$ to be some unknown coupling between the electrons and magnons, which is ultimately fixed by taking the classical limit [14,15].

Transforming to momentum space and using Fermi's golden rule, we obtain the interfacial spin current j_s^{int}, which can be expressed in terms of the real part of the spin mixing conductance per unit area $g_r^{\uparrow\downarrow}$ as [14,16]

$$j_s^{\mathrm{int}} = \frac{g_r^{\uparrow\downarrow}}{\pi s}\int d\varepsilon\, g(\varepsilon)(\varepsilon - \Delta\mu) \times\left[n_B\left(\frac{\varepsilon-\Delta\mu}{k_BT_e}\right) - n_B\left(\frac{\varepsilon-\mu_m}{k_BT_m}\right)\right]. \quad (1)$$

(Similar expressions were derived by Takahashi *et al.* [17] and Zhang and Zhang [18], although these are not given in terms of the spin-mixing conductance.)

Here s is the saturated spin density in the FI layer, $g(\varepsilon)$ is the magnon density of states, $n_B(x) = [e^x - 1]^{-1}$ is the Bose-Einstein distribution function, k_B is Boltzmann's constant, and T_m and T_e are the temperatures of the magnon and electron distributions, respectively, which we do not assume *a priori* to be equal (although the equal-temperature special case will be our primary interest). Of crucial importance in Eq. (1) are the magnon effective chemical potential μ_m—which we shall henceforth primarily refer to as the magnon spin accumulation—and the electron spin accumulation $\Delta\mu \equiv \mu^\uparrow - \mu^\downarrow$, which we define as the difference in chemical potentials for the spin-up and spin-down electrons. (In both cases, a positive accumulation means the majority of spin magnetic moments point in the $+y$ direction.)

We employ the magnon density of states,

$$g(\varepsilon) = \frac{\sqrt{\varepsilon-\Delta}}{4\pi^2 J_s^{\frac{3}{2}}}\Theta(\varepsilon-\Delta).$$

Here J_s is the spin wave stiffness constant, $\Theta(x)$ is the Heaviside step function, and Δ is the magnon gap, caused by a combination of external magnetic fields and internal anisotropy fields in ferromagnetic materials [19]. In our primary analysis of a Pt|YIG bilayer, we take $\Delta \equiv \mu_B \times 1\,\mathrm{T} \approx k_B \times 0.67\,\mathrm{K}$ with μ_B the Bohr magneton, in good agreement with, e.g., Cherepanov *et al.* [20], and in Sec. III E we specifically consider the limit of a vanishing magnon gap.

To treat the accumulations on equal footing, we now redefine $\mu_m \to \delta\mu_m$ and $\Delta\mu \to \delta\Delta\mu$, expand Eq. (1) to second order in δ, and set $\delta = 1$ to obtain

$$j_s^{\mathrm{int}} \simeq -\left[k_BT_mI_0 + I_e\Delta\mu + I_m\mu_m + \frac{I_{ee}}{k_BT_e}(\Delta\mu)^2 + \frac{I_{mm}}{k_BT_m}\mu_m^2 + \frac{I_{me}}{k_BT_m}\mu_m\Delta\mu\right]\frac{g_r^{\uparrow\downarrow}(k_BT_m)^{\frac{3}{2}}}{4\pi^3 J_s^{\frac{3}{2}}s}. \quad (2)$$

Here the I_i are dimensionless integrals given by Eqs. (A1) in the Appendix. All I_i are functions of T_m and Δ, and I_0, I_e,

TABLE I. System parameters for a Pt|YIG bilayer film.

Description	Symbol	Expression	Value at $T = 293\,\mathrm{K}$	Ref.
YIG spin-wave stiffness constant	J_s		$8.458 \times 10^{-40}\,\mathrm{J\,m^2}$	[21]
YIG spin quantum number per unit cell	S		10	[21]
YIG lattice constant	a		1.2376 nm	[21]
YIG Gilbert damping constant	α		1×10^{-4}	[21]
YIG spin number density	s	Sa^{-3}	$5.2754 \times 10^{27}\,\mathrm{m^{-3}}$	[21]
YIG magnon gap	Δ		$9.3 \times 10^{-24}\,\mathrm{J}$	[20]
YIG magnon-phonon scattering time	τ_{mp}		1 ps	[21]
YIG magnon relaxation time	τ_{mr}	$\frac{\hbar}{2\alpha k_B T_m}$	130 ps	[21]
Combined magnon relaxation time	τ	$\left(\frac{1}{\tau_{\mathrm{mr}}} + \frac{1}{\tau_{\mathrm{mp}}}\right)^{-1}$	1 ps	[21]
Magnon thermal de Broglie wavelength	Λ	$\sqrt{\frac{4\pi J_s}{k_B T_m}}$	1.62 nm	[21]
Magnon thermal velocity	v_{th}	$\frac{2\sqrt{J_s k_B T}}{\hbar}$	$35.1\,\mathrm{km\,s^{-1}}$	[21]
Magnon spin diffusion length	l_m	$v_{\mathrm{th}}\sqrt{\frac{2}{3}\tau\,\tau_{\mathrm{mr}}}$	326 nm	[21]
Magnon spin conductivity	σ_m	$\zeta\left(\frac{3}{2}\right)^2 \frac{J_s}{\Lambda^3}\tau$	$1.35 \times 10^{-24}\,\mathrm{J\,s\,m^{-1}}$	[21]
Real part of spin-mixing conductance	$g_r^{\uparrow\downarrow}$		$5 \times 10^{18}\,\mathrm{m^{-2}}$	[16]
Pt electrical conductivity	σ		$1 \times 10^{7}\,\mathrm{S\,m^{-1}}$	[23][a]
Pt spin Hall angle	θ_{SH}		0.11	[21]
Pt electron diffusion length	l_s		1.5 nm	[21]
Pt|YIG Kapitza resistance	R_{th}		$3.58 \times 10^{-9}\,\mathrm{m^2\,K\,W^{-1}}$	[25]

[a]The conductivity of Pt is approximately inverse-linear in temperature over the regime we are considering. However, as we are not interested in detailed thermodynamic behavior, we use the fixed value $\sigma = 1 \times 10^7\,\mathrm{S\,m^{-1}}$ throughout this work.

and I_{ee} additionally depend on T_e. In the special case where $T_m = T_e$, I_0 vanishes, $I_m = -I_e$, and $I_{ee} = -(I_{mm} + I_{me})$.

In addition to j_s^{int}, the spin accumulations and the electric driving field E give rise to the following spin currents in the z direction:

$$j_s^e = \frac{\hbar}{2e}\left(-\frac{\sigma}{2e}\frac{\partial \Delta\mu}{\partial z} - \sigma\theta_{\mathrm{SH}}E\right), \tag{3a}$$

$$j_s^m = -\frac{\sigma_m}{\hbar}\frac{\partial \mu_m}{\partial z}. \tag{3b}$$

Here j_s^e and j_s^m are the electron and magnon spin currents, respectively. σ is the electrical conductivity in the HM, σ_m is the magnon conductivity in the ferromagnet, e is the elementary charge, and θ_{SH} is the spin Hall angle.

In line with Cornelissen *et al.* [21] and Zhang and Zhang [22], we assume the spin accumulations μ_m and $\Delta\mu$ obey diffusion equations along the z axis:

$$\frac{d^2\mu_m}{dz^2} = \frac{\mu_m}{l_m^2}, \quad \frac{d^2\Delta\mu}{dz^2} = \frac{\Delta\mu}{l_e^2},$$

where l_m and l_e are the magnon and electron diffusion lengths, respectively. We solve these equations analytically subject to boundary conditions that demand continuity of the spin current across the interface and confinement of the currents to the sample:

$$j_s^m(0) = j_s^e(0) = j_s^{\mathrm{int}}(0),$$
$$j_s^m(L_{\mathrm{FI}}) = j_s^e(-L_{\mathrm{HM}}) = 0.$$

This system of equations now fully specifies the magnonic and electronic spin accumulations μ_m and $\Delta\mu$, the latter of which enters the charge current j_c via the spin Hall effect:

$$j_c(z) = \sigma E + \frac{\sigma\theta_{\mathrm{SH}}}{2e}\frac{\partial\Delta\mu(z)}{\partial z}. \tag{4}$$

The measured resistivity at some electric field strength E is then given by the ratio of the electric field and the averaged charge current:

$$\rho(E) = \frac{E}{\frac{1}{L_{\mathrm{HM}}}\int_{-L_{\mathrm{HM}}}^{0} dz\, j_c(z)}. \tag{5}$$

Finally, we define the USMR $\mathcal{U}$ as the fractional difference in resistivity on inverting the electric field:

$$\mathcal{U} \equiv \left|\frac{\rho(E) - \rho(-E)}{\rho(E)}\right| = \left|1 + \frac{\int_{-L_{\mathrm{HM}}}^{0} dz\, j_c(z;E)}{\int_{-L_{\mathrm{HM}}}^{0} dz\, j_c(z;-E)}\right|.$$

It should be noted that the even-ordered terms in the expansion of the interface current are vital to the appearance of unidirectional SMR. Suppose our system has equal magnon and electron temperature, such that the interfacial spin Seebeck term I_0 vanishes (see Sec. III B), and we ignore the quadratic terms in Eq. (2). Then because the only term in the spin current equations (3) that is independent of the accumulations is $-\frac{\hbar\sigma\theta_{\mathrm{SH}}}{2e}E$ in Eq. (3a), we have that $\Delta\mu \propto \mu_m \propto E$. Then by Eqs. (4) and (5), $j_c \propto E$ and $\rho(E) \propto \frac{E}{E}$, such that $\mathcal{U} = 0$. Conversely, with quadratic terms in the interfacial spin current, $\rho(E) \sim \frac{E}{E+E^2}$, and likewise if I_0 does not vanish, $\rho(E) \sim \frac{E}{1+E}$. Both cases give nonvanishing USMR. Physically, one can say that the spin-dependent electron and magnon populations couple together in a nonlinear fashion [namely through the Bose-Einstein distributions in Eq. (1)], leading to a nonlinear dependence on the electric field.

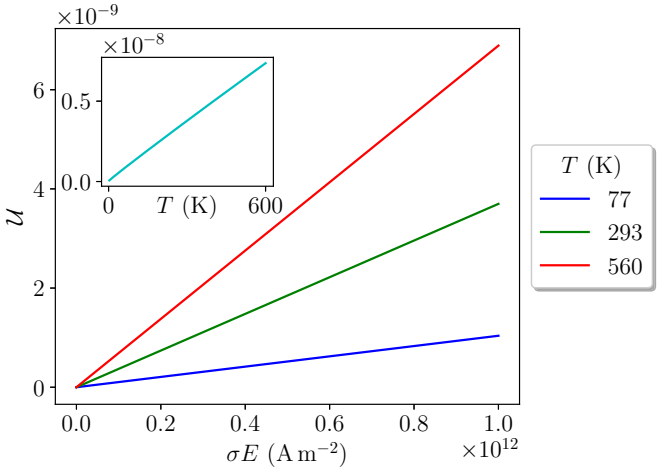

FIG. 2. USMR $\mathcal{U}$ versus driving current σE for a Pt|YIG bilayer at liquid nitrogen temperature (77 K, blue), room temperature (293 K, green), and the YIG Curie temperature (560 K, red). Inset: USMR versus system temperature T at fixed current $\sigma E = 1 \times 10^{12}\,\mathrm{A\,m^{-2}}$.

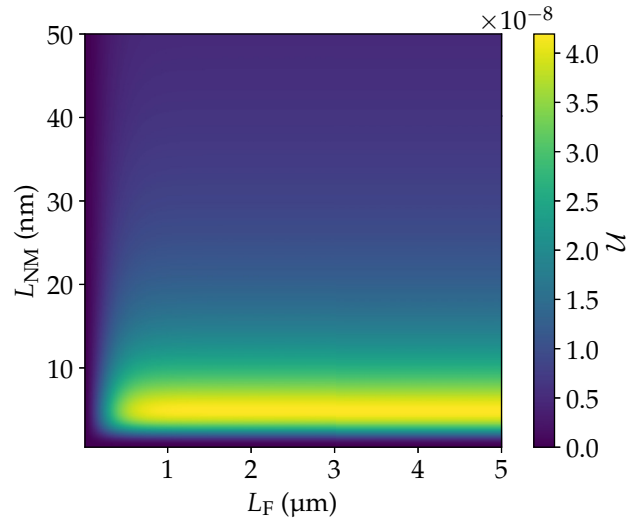

FIG. 3. Pt|YIG USMR $\mathcal{U}$ at $T_m = T_e = 293\,\mathrm{K}$ versus FI layer thickness L_{FI} and HM layer thickness L_{HM}. A driving current $\sigma E = 1 \times 10^{12}\,\mathrm{A\,m^{-2}}$ is used. A maximal USMR of 4.2×10^{-8} is reached at $L_{\mathrm{HM}} = 4.5\,\mathrm{nm}$, $L_{\mathrm{FI}} = 5\,\mu\mathrm{m}$.

III. RESULTS

A. Equal-temperature, finite-gap case

Although our model can be solved analytically (up to evaluation of the integrals I_i), the full expression of $\mathcal{U}$ is unwieldy and therefore hardly insightful. To get an idea of the behavior of a real system, we use a set of parameters—listed in Table I—corresponding to a Pt|YIG bilayer as a starting point. (Unless otherwise specified, all parameters used henceforth are to be taken from this table.)

Figure 2 shows the magnonic USMR of a Pt|YIG bilayer versus applied driving current (σE) when $T_m = T_e = T$ at the temperature of liquid nitrogen (77 K, blue), room temperature (293 K, green), and the Curie temperature of YIG (560 K [20], red). The FI and HM layer thicknesses used are 90 nm and 3 nm, respectively, in line with experimental measurements by Avci *et al.* [24].

In all cases the magnonic USMR is proportional to the applied electric current—that is, the cubic term found by Avci *et al.* [10] is absent and at room temperature has a value on the order of 10^{-9} at typical measurement currents [4]. This is roughly four orders of magnitude weaker than the USMR obtained—both experimentally and theoretically—for FM|HM hybrids [4,6,8,24] and is consistent with the experimental null results obtained for this system by Avci *et al.* [24]. Note, however, that the thickness of the FI layer used by these authors is significantly lower than the magnon spin diffusion length $l_m = 326\,\mathrm{nm}$, which results in a suppressed USMR.

Furthermore, it can be seen in the inset of Fig. 2 that the magnonic USMR is, to good approximation, linear in the system temperature, in agreement with observations by Kim *et al.* [9] and Avci *et al.* [10].

In Fig. 3 we compute the USMR at $\sigma E = 1 \times 10^{12}\,\mathrm{A\,m^{-2}}$ as a function of both L_{FI} and L_{HM}. A maximum is reached around $L_{\mathrm{HM}} \approx 4.5\,\mathrm{nm}$, while in terms of L_{FI}, a plateau is approached within a few spin diffusion lengths. By varying the layer thicknesses, a maximal USMR of 4.2×10^{-8} can be achieved, an improvement of one order of magnitude compared to the thicknesses used by Avci *et al.* [24].

B. Thermal effects

We take into account a difference between the electron and magnon temperatures T_e and T_m by assuming these parameters are equal to the temperatures of the HM and FI layers, respectively, which we take to be homogeneous. We assume that the HM undergoes ohmic heating and dissipates this heat into the ferromagnet, which we take to be an infinite heat bath at temperature T_m. We only take into account the interfacial (Kapitza) thermal resistance R_{th} between the HM and FI layers, leading to a simple expression for the HM temperature T_e:

$$T_e = T_m + R_{\mathrm{th}} \sigma E^2 L_{\mathrm{HM}}.$$

Using this model, we still find a linear dependence in the electric field, $\mathcal{U} \simeq u_E(T_m)\sigma E$, but the coefficient $u_E(T_m)$ increases by three orders of magnitude compared to the case where the electron and magnon temperatures are set to be equal. The overwhelming majority of this increase can be attributed to an interfacial spin Seebeck effect (SSE) [21,25]: It is caused by the accumulation-independent contribution I_0 [Eq. (A1a)] in the interface current. When I_0 is artificially set to 0, $u_E(T_m)$ changes less than 1% from its equal-temperature value.

Furthermore, the overall magnitude of the interfacial SSE in our system can be attributed to the fact that we have a conductor|insulator interface: The current runs through the HM only, resulting in inhomogeneous Joule heating of the sample and a large temperature discontinuity across the interface.

C. Spin Hall angle

The electronic spin accumulation $\Delta\mu$ at the interface in the standard spin Hall effect is linear in the electric field E and spin Hall angle θ_{SH} [3]. From the linearity in E, we may

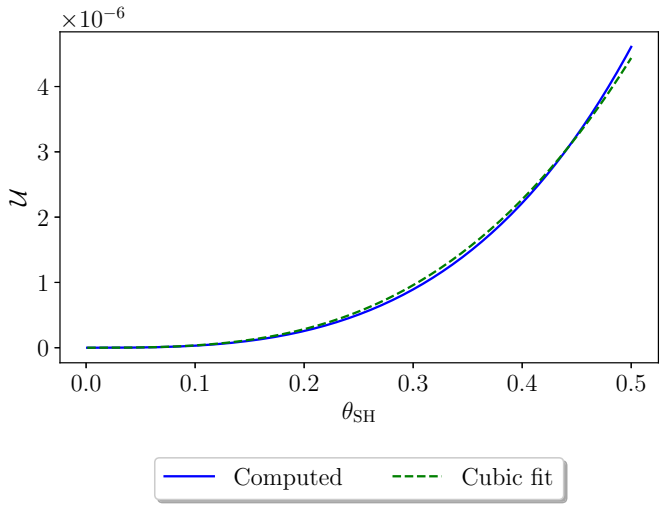

FIG. 4. USMR $\mathcal{U}$ at $T_m = T_e = 293\,\mathrm{K}$ versus spin Hall angle θ_{SH}. A driving current $\sigma E = 1 \times 10^{12}\,\mathrm{A\,m^{-2}}$ and FI and HM layer thicknesses $L_{\mathrm{FI}} = 5\,\mu\mathrm{m}$ and $L_{\mathrm{HM}} = 4.5\,\mathrm{nm}$ are used. Blue curve: Computed value. Dashed green curve: Fit of the form $\mathcal{U} = u_\theta \theta_{\mathrm{SH}}^3$, with $u_\theta \simeq 3.1 \times 10^{-4}$.

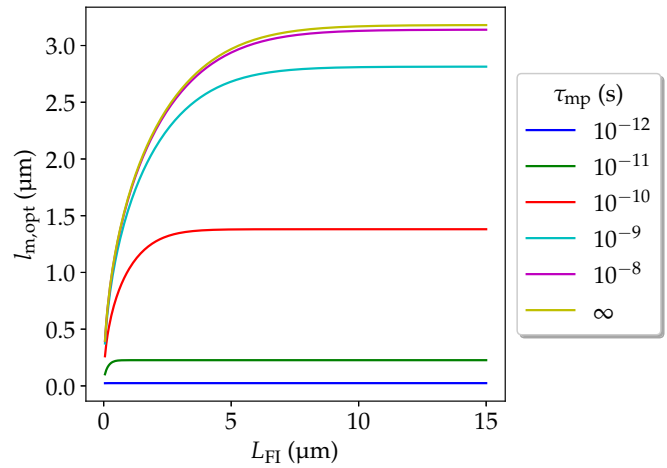

FIG. 5. Value of the magnon spin diffusion length l_m that maximizes the USMR, as a function of FI layer thickness L_{FI}, at various values of the magnon-phonon relaxation time τ_{mp}.

conclude that the terms in Eq. (2) that are linear in $\Delta\mu$ have a suppressed contribution to the USMR. Thus, the contribution of the interface current is of order θ_{SH}^2. Furthermore, $\Delta\mu$ enters the charge current [Eq. (4)] with a prefactor θ_{SH}, leaving the magnonic USMR predominantly cubic in the spin Hall angle. Indeed, in the special case $T_m = T_e$, expanding the full expression for $\mathcal{U}$ (which spans several pages and is therefore not reproduced within this work) in θ_{SH} reveals that the first nonzero coefficient is that of θ_{SH}^3. This suggests a small change in θ_{SH} potentially has a large effect on the USMR.

In Fig. 4 we plot the USMR for a Pt|YIG bilayer—once again using $T_m = T_e = 293\,\mathrm{K}$—consisting of 4.5 nm of Pt and 5 μm of YIG, in which we sweep the spin Hall angle. Included is a cubic fit $\mathcal{U} = u_\theta \theta_{\mathrm{SH}}^3$, where we find $u_\theta \simeq 3.1 \times 10^{-4}$. Here it can be seen that the magnonic USMR in HM|FI bilayers can, as expected, potentially acquire magnitudes roughly comparable to those in HM|FM systems, provided one can find or engineer a metal with a spin Hall angle several times greater than that of Pt. This suggests that very strong spin-orbit coupling (SOC) is liable to produce significant magnon-mediated USMR in FI|HM heterostructures, although we expect our model to break down in this regime.

D. A note on the magnon spin diffusion length

Although we use the analytic expression for the magnon spin diffusion length [18,21,22],

$$l_m = v_{\mathrm{th}} \sqrt{\frac{2}{3} \tau \tau_{\mathrm{mr}}}$$

where v_{th} is the magnon thermal velocity, τ is the combined relaxation time, and τ_{mr} is the magnonic relaxation time (see Table I)—this is known to correspond poorly to reality, being at least an order of magnitude too low in the case of YIG [21]. Artificially setting the magnon spin-diffusion length to the experimental value of 10 μm (while otherwise continuing to use the parameters from Table I) results in a drop in USMR of some four orders of magnitude.

It follows directly that there exists some optimal value of l_m (which we shall label $l_{m,\mathrm{opt}}$) that maximizes the USMR, which we plot as a function of the FI layer thickness L_{FI} in Fig. 5, at $L_{\mathrm{HM}} = 4.5\,\mathrm{nm}$ and $\sigma E = 1 \times 10^{12}\,\mathrm{A\,m^{-2}}$, and for various values of the magnon-phonon relaxation time τ_{mp}, which is the shortest and therefore most important timescale we take into account. For the physically realistic value of $\tau_{\mathrm{mp}} = 1\,\mathrm{ps}$ (blue curve), the optimal magnon spin diffusion length is just 24 nm. Although $l_{m,\mathrm{opt}}$ itself depends on τ_{mp}, the condition $l_m = l_{m,\mathrm{opt}}$ acts to cancel the dependence of the USMR on the magnon-phonon relaxation time. Curiously, the USMR additionally loses its dependence on L_{FI}, reaching a fixed value of 4.14×10^{-7} for our parameters.

We further find that $l_{m,\mathrm{opt}}$ is independent of the spin Hall angle and driving current and shows a weak decrease with increasing temperature provided the magnon-phonon scattering time is sufficiently short. A significant increase in the optimal spin diffusion length is only found at low temperatures and large τ_{mp}. Similarly, a weak dependence on the Gilbert damping constant α is found, becoming more significant at large τ_{mp}, with lower values of α corresponding to larger $l_{m,\mathrm{opt}}$. When α is swept, again the USMR at $l_m = l_{m,\mathrm{opt}}$ acquires a universal value of 4.14×10^{-7} for our system parameters.

E. Effect of the magnon gap

We have thus far utilized a fixed magnon gap with a value of $\Delta/\mu_B = 1\,\mathrm{T}$ for YIG. Although this is reasonable for typical systems, it is possible to significantly reduce the gap size by minimizing the anisotropy fields within the sample, e.g., using a combination of external fields [26], optimized sample shapes [19,27], and temperature [28,29]. This leads us to consider the effect a decreased or even vanishing gap may have on our results.

Figure 6 shows the USMR $\mathcal{U}$ for a Pt|YIG system (4.5 nm of Pt and 5 μm of YIG) at room temperature, plotted against the driving current σE, now for different values of the magnon

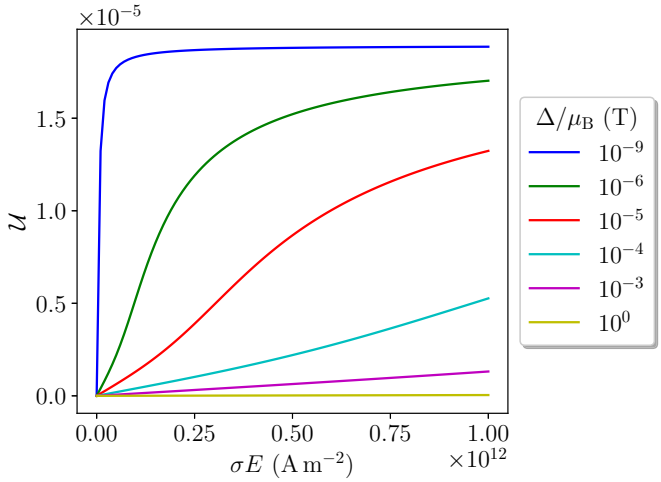

FIG. 6. USMR $\mathcal{U}$ of a Pt(4.5 nm)|YIG(5μm) bilayer at room temperature versus applied current σE at various values of the magnon gap Δ. For large gaps, linear behavior is recovered at realistic currents, while for smaller gap sizes, the USMR saturates as the current is increased.

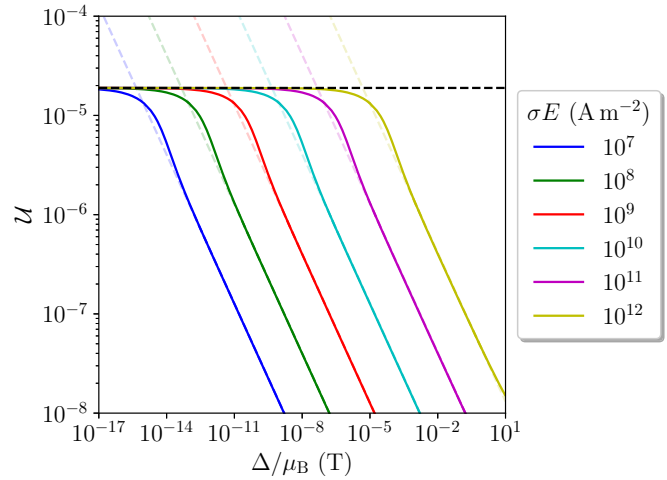

FIG. 7. USMR $\mathcal{U}$ of a Pt(4.5 nm)|YIG(5 μm) bilayer at room temperature as function of the magnon gap size Δ for various values of the base charge current σE. Note the log-log scaling. Solid colored lines: Computed USMR. Dashed colored lines: Continuations of the high-gap tails of the corresponding curves according to the one-parameter fit $\mathcal{U} = u_0/\sqrt{\Delta}$. Dashed black line: asymptotic value of the USMR as given by Eq. (6).

gap Δ. Here it can be seen that while $\mathcal{U}$ is linear in E for large gap sizes and realistic currents, it shows limiting behavior at smaller gaps, becoming independent of the electric current above some threshold (provided one neglects the effect of Joule heating). At low current and intermediate magnon gap, the current dependence is nonlinear at $\mathcal{O}(I^2)$ as opposed to the $\mathcal{O}(I^3)$ behavior found by Avci *et al.* [10].

Note also that the saturation value of the USMR is two to three orders of magnitude greater than the values found previously in our work, and of the same magnitude as the electronic contribution found by Zhang and Vignale [8].

The maximal value of the USMR that can be achieved may be found by considering the full analytic expression for $\mathcal{U}$ in terms of the generic coefficients I_i representing the dimensionless integrals given by Eqs. (A1) in the Appendix. In the gapless limit $\Delta \to 0$ and at equal magnon and electron temperature ($T_m = T_e$), the second-order coefficients I_{mm} and I_{me} diverge, while their sum takes the constant value $\lambda \equiv I_{mm} + I_{me} \simeq 0.323551$ at room temperature. I_{ee} does not diverge, and obtains the value $-\lambda$.

Now working in the thick-ferromagnet limit ($L_{\mathrm{FI}} \to \infty$), we substitute $I_{me} \to -I_{mm} + \lambda$ and take the limits $E \to \infty$ and $I_{mm} \to -\infty$. By application of l'Hôpital's rule in the latter, all coefficients I_i drop out of the expression for $\mathcal{U}$. This leaves only the asymptotic value, which, after expanding in θ_{SH}, reads

$$\mathcal{U}_{\max} = \frac{4e^2 l_s^2 \theta_{\mathrm{SH}}^2 \sigma_m \tanh^2\left(\frac{L_{\mathrm{HM}}}{2l_s}\right)}{\hbar^2 l_m L_{\mathrm{HM}} \sigma + 4 l_s e^2 L_{\mathrm{HM}} \sigma_m \coth\left(\frac{L_{\mathrm{HM}}}{l_s}\right)} + \mathcal{O}\left(\theta_{\mathrm{SH}}^4\right). \quad (6)$$

Whereas the linear-in-E regime of the magnonic USMR grows as θ_{SH}^3, we thus find that the leading-order behavior of the *asymptotic* value is only θ_{SH}^2, and the third-order term vanishes completely. Physically, this can be explained by the fact that the asymptotic magnonic USMR is purely a bulk effect: All details about the interface vanish, while parameters originating from the bulk spin and charge currents remain. The appearance of l_m in the denominator and its absence in the numerator of Eq. (6) once again highlights that a large magnon spin diffusion length acts to *suppress* the USMR.

Figure 7 is a log-log plot of the USMR versus gap size Δ at various values of the driving current σE. Here the value $\mathcal{U}_{\max}$ is shown as a dashed black line, indicating that this is indeed the value to which $\mathcal{U}$ converges in the gapless limit or at high current. Moreover, it shows that for given σE, one can find a turning point at which the USMR switches relatively abruptly from being nearly constant to decreasing as $1/\sqrt{\Delta}$.

A (backward) continuation of the decreasing tails is included in Fig. 7 as dashed lines following the one-parameter fit $\mathcal{U} = u_0/\sqrt{\Delta}$, and we define the threshold gap Δ_{th} as the value of Δ where this continuation intersects $\mathcal{U}_{\max}$. We then find that Δ_{th} scales as E^2, or conversely, that the driving current required to saturate the USMR scales as the square root of the magnon gap.

We note that although the small-gap regime is mathematically valid (even in the limit $\Delta \to 0$, as Δ may be brought arbitrarily close to 0 in a continuous manner), it does not necessarily correspond to a physical situation: When the anisotropy vanishes, the magnetization of the FI layer may be reoriented freely, which will break our initial assumptions. Nevertheless, in taking the gapless limit, we are able to predict an upper limit on the magnonic USMR.

IV. CONCLUSIONS

Using a simple drift-diffusion model, we have shown that magnonic spin accumulation near the interface between a ferromagnetic insulator and a heavy metal leads to a small but nonvanishing contribution to the unidirectional spin Hall magnetoresistance of FI|HM heterostructures. Central to our model is an interfacial spin current originating from a spin-flip scattering process whereby electrons in the heavy metal

create or annihilate magnons in the ferromagnet. This current is markedly nonlinear in the electronic and magnonic spin accumulations at the interface, and it is exactly this nonlinearity which gives rise to the magnonic USMR.

For Pt|YIG bilayers, we predict that the magnonic USMR $\mathcal{U}$ is at most on the order of 10^{-8}, roughly three orders of magnitude weaker than the measured USMR in FM|HM hybrids (where electronic spin accumulation is thought to form the largest contribution). This is fully consistent with experiments that fail to detect USMR in Pt|YIG systems, as the tiny signal is drowned out by the interfacial spin Seebeck effect, which has a similar experimental signature and is enhanced compared to the FM|HM case due to inhomogeneous Joule heating.

We have shown that the magnon-mediated USMR is approximately cubic in the spin Hall angle of the metal, suggesting that metals with extremely large spin Hall angles may provide a significantly larger USMR than Pt. It is therefore plausible that a large magnonic USMR can exist in systems with very strong spin-orbit coupling, even though our model would break down in this regime.

The magnonic USMR depends strongly on the magnon spin diffusion length l_m in the ferromagnet. Motivated by a large discrepancy between experimental values and theoretical predictions of l_m, we have shown that a significant increase in USMR can be realized if a method is found to engineer this parameter to specific, optimal values that, for realistic values of the magnon-phonon relaxation time τ_{mp} (on the order of 1 ps for YIG), are significantly shorter than those measured experimentally or computed theoretically. We further find that when the magnon spin diffusion length has its optimal value, the USMR becomes independent of the ferromagnet's thickness and Gilbert damping constant.

Although in physically reasonable regimes the magnonic USMR is to very good approximation linear in the applied driving current σE, it saturates to a fixed value given extremely large currents or a strongly reduced magnon gap Δ. The transition from linear to constant behavior in the driving current is heralded by a turning point which is proportional to the square root of the magnon gap. The asymptotic behavior of the USMR beyond the turning point is governed by the bulk spin and charge currents and is completely independent of the details of the interface.

While a vast reduction in Δ is required to bring the saturation current of a Pt|YIG bilayer within experimentally reasonable regimes, the magnonic USMR scales as $1/\sqrt{\Delta}$ at currents below the turning point, suggesting that highly isotropic FI|HM samples are most likely to produce a measurable magnonic USMR. The increase in magnonic USMR at low gaps (and large currents) is in good qualitative agreement with the recent experimental work of Avci *et al.* [10], as is the linear dependence on system temperature.

A notable disagreement with the experimental data of Avci *et al.* [10] is found in the scaling of the current dependence, which in our results lacks an $\mathcal{O}(I^3)$ term at large magnon gaps and contains an $\mathcal{O}(I^2)$ term at intermediate gaps. It is still unclear whether this discrepancy can be explained by system differences, such as the finite electrical resistance of Co or the presence of Joule heating.

Finally, we note that while our results apply to ferromagnetic insulators, it is reasonable to assume a magnonic contribution also exists in HM|FM heterostructures, although the possibility of coupled transport of magnons and electrons makes such systems more difficult to model. Additionally, various extensions of our model may be considered, such as the incorporation of spin-momentum locking [5], ellipticity of magnons, heat transport and nonuniform temperature profiles [21], directional dependence of the magnetization, etc.

ACKNOWLEDGMENTS

R.A.D. is member of the D-ITP consortium, a program of the Dutch Organisation for Scientific Research (NWO) that is funded by the Dutch Ministry of Education, Culture and Science (OCW). This work is funded by the European Research Council (ERC).

APPENDIX: INTERFACIAL SPIN CURRENT INTEGRALS

The following dimensionless integrals appear in the second-order expansion of the interfacial spin current to the spin accumulations, Eq. (2):

$$I_0 = \int_{\frac{\Delta}{k_B T_m}}^{\infty} dx \sqrt{x - \frac{\Delta}{k_B T_m}} x \left[n_B(x) - n_B\left(\frac{T_m}{T_e} x\right) \right], \tag{A1a}$$

$$I_e = \int_{\frac{\Delta}{k_B T_m}}^{\infty} dx \sqrt{x - \frac{\Delta}{k_B T_m}} \left\{ n_B\left(\frac{T_m}{T_e} x\right) - n_B(x) - \frac{T_m}{T_e} x e^{\frac{T_m}{T_e} x} \left[n_B\left(\frac{T_m}{T_e} x\right) \right]^2 \right\}, \tag{A1b}$$

$$I_m = \int_{\frac{\Delta}{k_B T_m}}^{\infty} dx \sqrt{x - \frac{\Delta}{k_B T_m}} x e^x [n_B(x)]^2, \tag{A1c}$$

$$I_{ee} = \int_{\frac{\Delta}{k_B T_m}}^{\infty} dx \sqrt{x - \frac{\Delta}{k_B T_m}} \left\{ e^{\frac{T_m}{T_e} x} \left[n_B\left(\frac{T_m}{T_e} x\right) \right]^3 \times \left[e^{\frac{T_m}{T_e} x} - 1 - \frac{T_m x}{2 T_e} \left(e^{\frac{T_m}{T_e} x} + 1 \right) \right] \right\}, \tag{A1d}$$

$$I_{mm} = \int_{\frac{\Delta}{k_B T_m}}^{\infty} dx \sqrt{x - \frac{\Delta}{k_B T_m}} \frac{x}{2} e^x [e^x + 1] [n_B(x)]^3, \tag{A1e}$$

$$I_{me} = -\int_{\frac{\Delta}{k_B T_m}}^{\infty} dx \sqrt{x - \frac{\Delta}{k_B T_m}} e^x [n_B(x)]^2. \tag{A1f}$$

[1] T. McGuire and R. Potter, IEEE Trans. Magn. **11**, 1018 (1975).

[2] G. Binasch, P. Grünberg, F. Saurenbach, and W. Zinn, Phys. Rev. B **39**, 4828 (1989).

[3] Y.-T. Chen, S. Takahashi, H. Nakayama, M. Althammer, S. T. B. Goennenwein, E. Saitoh, and G. E. W. Bauer, Phys. Rev. B **87**, 144411 (2013).
[4] C. O. Avci, K. Garello, A. Ghosh, M. Gabureac, S. F. Alvarado, and P. Gambardella, Nat. Phys. **11**, 570 (2015).
[5] K. Yasuda, A. Tsukazaki, R. Yoshimi, K. S. Takahashi, M. Kawasaki, and Y. Tokura, Phys. Rev. Lett. **117**, 127202 (2016).
[6] Y. Yin, D.-S. Han, M. C. H. de Jong, R. Lavrijsen, R. A. Duine, H. J. M. Swagten, and B. Koopmans, Appl. Phys. Lett. **111**, 232405 (2017).
[7] C. O. Avci, M. Mann, A. J. Tan, P. Gambardella, and G. S. D. Beach, Appl. Phys. Lett. **110**, 203506 (2017).
[8] Steven S.-L. Zhang and G. Vignale, Phys. Rev. B **94**, 140411 (2016).
[9] K. J. Kim, T. Moriyama, T. Koyama, D. Chiba, S. W. Lee, S. J. Lee, K. J. Lee, H. W. Lee, and T. Ono, arXiv:1603.08746 [cond-mat.mtrl-sci].
[10] C. O. Avci, J. Mendil, G. S. D. Beach, and P. Gambardella, Phys. Rev. Lett. **121**, 087207 (2018).
[11] E. M. Chudnovsky, Phys. Rev. Lett. **99**, 206601 (2007).
[12] W. Zhang, W. Han, X. Jiang, S.-H. Yang, and S. S. P. Parkin, Nat. Phys. **11**, 496 (2015).
[13] T. Holstein and H. Primakoff, Phys. Rev. **58**, 1098 (1940).
[14] S. A. Bender and Y. Tserkovnyak, Phys. Rev. B **91**, 140402 (2015).
[15] Y. Tserkovnyak, A. Brataas, and G. E. W. Bauer, Phys. Rev. Lett. **88**, 117601 (2002).
[16] S. A. Bender, R. A. Duine, and Y. Tserkovnyak, Phys. Rev. Lett. **108**, 246601 (2012).
[17] S. Takahashi, E. Saitoh, and S. Maekawa, in *Journal of Physics Conference Series*, Vol. 200 (IOP Publishing, Bristol, UK, 2010), p. 062030.
[18] Steven S.-L. Zhang and S. Zhang, Phys. Rev. B **86**, 214424 (2012).
[19] C. Tang, M. Aldosary, Z. Jiang, H. Chang, B. Madon, K. Chan, M. Wu, J. E. Garay, and J. Shi, Appl. Phys. Lett. **108**, 102403 (2016).
[20] V. Cherepanov, I. Kolokolov, and V. L'vov, Phys. Rep. **229**, 81 (1993).
[21] L. J. Cornelissen, K. J. H. Peters, G. E. W. Bauer, R. A. Duine, and B. J. van Wees, Phys. Rev. B **94**, 014412 (2016).
[22] Steven S.-L. Zhang and S. Zhang, Phys. Rev. Lett. **109**, 096603 (2012).
[23] *ASM Handbook Committee* (ASM International, Materials Park, OH, 1990), Vol. 2, p. 688, https://www.asminternational.org/search/-/journal_content/56/10192/06182G/PUBLICATION.
[24] C. O. Avci, K. Garello, J. Mendil, A. Ghosh, N. Blasakis, M. Gabureac, M. Trassin, M. Fiebig, and P. Gambardella, Appl. Phys. Lett. **107**, 192405 (2015).
[25] M. Schreier, A. Kamra, M. Weiler, J. Xiao, G. E. W. Bauer, R. Gross, and S. T. B. Goennenwein, Phys. Rev. B **88**, 094410 (2013).
[26] M. G. Pini, P. Politi, and R. L. Stamps, Phys. Rev. B **72**, 014454 (2005).
[27] H. Skarsvåg, C. Holmqvist, and A. Brataas, Phys. Rev. Lett. **115**, 237201 (2015).
[28] J. F. Dillon, Phys. Rev. **105**, 759 (1957).
[29] G. P. Rodrigue, H. Meyer, and R. V. Jones, J. Appl. Phys. **31**, S376 (1960).